(13) D. K. Lavallee, J. G. Brace, and N. Winograd, *Inorg. Chem.*, **18**, 1776 (1979).
(14) J. P. Macquet, M. M. Millard, and T. Theophanides, *J. Am. Chem. Soc.*, **100**, 4741 (1978).
(15) S. Kitagawa, I. Morishima, T. Yonezawa, and N. Sato, *Inorg. Chem.*, **18**, 1345 (1979).
(16) J. L. Hoard, *Science*, **174**, 1295 (1971).
(17) J. J. Katz and T. R. Janson, *Ann. N.Y. Acad. Sci.*, **206**, 579 (1973).
(18) C. B. Storm and Y. Teklu, *J. Am. Chem. Soc.*, **94**, 1745 (1972).
(19) A. D. Adler, F. R. Longo, and V. Varadi, *Inorg. Synth.*, **16**, 213–220 (1976).
(20) D. H. Dolphin, J. R. Sams, and T. B. Tsin, *Inorg. Chem.*, **16**, 711 (1977).
(21) K. M. Kadish, L. A. Bottomley, and J. S. Cheng, *J. Am. Chem. Soc.*, **100**, 2731 (1978).
(22) C. D. Wagner, "Energy Calibration of Electron Spectrometers", in press, and references cited therein.
(23) G. M. Bancroft, I. Adams, H. Lampe, and T. K. Shaw, *J. Electron Spectrosc. Relat. Phenom.*, **9**, 191 (1976).
(24) K. M. Kadish, L. A. Bottomley, and D. Schaeper, submitted for publication.
(25) H. Goff, private communication.
(26) C. A. Reed, T. Mashiko, S. P. Bentley, M. E. Kastner, W. R. Scheidt, K. Spartalion, and G. Lang, *J. Am. Chem. Soc.*, **101**, 2948 (1979).
(27) T. A. Carlson, "Photoelectron and Auger Spectroscopy", Plenum Press, New York, 1975.
(28) R. P. Gupta and S. K. Sen, *Phys. Rev. B*, **10**, 71 (1974).
(29) M. M. Maltempo, *Q. Rev. Biophys.*, **9**, 181 (1976).
(30) D. N. Henrickson, J. M. Hollander, and W. L. Jolly, *Inorg. Chem.*, **8**, 2642 (1969).
(31) Reference 27, p 235.
(32) TPPFeNO as reported by W. R. Scheidt and M. E. Frisse, *J. Am. Chem. Soc.*, **97**, 17 (1975).

# On the Mechanism of Autoxidation of Iron(II) Porphyrins. Detection of a Peroxo-Bridged Iron(III) Porphyrin Dimer and the Mechanism of Its Thermal Decomposition to the Oxo-Bridged Iron(III) Porphyrin Dimer

**Der-Hang Chin, Gerd N. La Mar,* and Alan L. Balch***

*Contribution from the Department of Chemistry, University of California, Davis, California 95616.* *Received October 29, 1979*

**Abstract:** Addition of dioxygen to toluene solutions of $Fe^{II}P$ (P = a porphyrin dianion) at −80 °C leads to the formation of a new intermediate **1** which has been detected by visible and $^1H$ NMR spectroscopy. **1** reacts quantitatively with $Fe^{II}P$ according to the equation $\mathbf{1} + 2Fe^{II}P \rightarrow 2PFeOFeP$. A peroxo-bridged, dimeric structure, $PFe^{III}$-O-O-$Fe^{III}P$, is proposed for **1** on the basis of its composition, its antiferromagnetism (as determined by the temperature dependence of the $^1H$ NMR contact shifts and the magnetic susceptibility, 2.1 $\mu_B$ at 181 K, 2.7 $\mu_B$ at 224 K) and the detection of a mixed ligand species involving two differently substituted porphyrins. Upon warming **1** decomposes quantitatively by the reaction $2\ \mathbf{1} \rightarrow 2PFeOFeP + O_2$ with no other species detected during the reaction. The dioxygen produced has been detected by mass spectroscopy and by its reaction with $Fe^{II}P$. The kinetics of this reaction have been determined over the temperature range −22 to −40 °C. The reaction is first order in **1** with $\Delta H^{\ddagger} = 14.5 \pm 1$ kcal/mol and $\Delta S^{\ddagger} = -15 \pm 1$ eu. Isotopic labeling of the dioxygen used to form **1** reveals that the isotopic composition of the $O_2$ released due to decomposition of **1** is identical with that used in its formation. However, when two labeled species $PFeO_2FeP$ and $P'FeO_2FeP'$ are decomposed, the porphyrin ligands do scramble: PFeOFeP, P′FeOFeP′, and PFeOFeP′ all are formed. Based on these observations, a mechanism for the decomposition of **1** to PFeOFeP is proposed.

## Introduction

The interaction of dioxygen with $Fe^{II}$ compounds, particularly $Fe^{II}$ porphyrins, has received considerable attention because of its relevance to the physiological problems of dioxygen transport, storage, and utilization. Autoxidation of simple $Fe^{II}$ porphyrins, as well as other iron complexes, produces $\mu$-oxo $Fe^{III}$ dimers via the stoichiometry[1]

$$4Fe^{II} + O_2 \rightarrow 2Fe^{III}\text{-}O\text{-}Fe^{III} \qquad (1)$$

Several studies have indicated that the reaction 1 exhibits kinetic behavior which is first order in dioxygen and second order in $Fe^{II}$ complex.[2-4] Consequently, a bridged FeOOFe species, variously described as $Fe^{II}$-$O_2$-$Fe^{II}$ (dioxygen bridge)[3,5] or $Fe^{III}$-$O_2$-$Fe^{III}$ (peroxo bridge),[3] has been postulated to form during the initial stages of autoxidation. However, very little is known about the structure, properties, and chemical reactivity of these postulated FeOOFe complexes. Prior to the work described here, the only cases of observation of adducts of the stoichiometry $Fe_2O_2$ were in the crustacean respiratory pigment hemerythrin[6] and the oxygenation of a synthetic iron macrocyclic complex.[7] However, for other metals ample precedent exists for the formation of MOOM units. The formation of $Co^{III}$-O-O-$Co^{III}$ units by oxygenation of $Co^{II}$ complexes is particularly well documented.[8] Although FeOOFe units have long remained undetected, their probable existence has exerted an influence on the synthetic chemistry involved in constructing models for the reversible dioxygen binding sites of the hemoglobins and myoglobins. In several cases, particularly in the various strapped and picket-fence porphyrins, steric bulk has been built into the iron-binding macrocycles so that the close approach is effectively prohibited.[7,10]

Because of the difficulty in detecting the FeOOFe unit, the mechanism of its conversion into the final product, the $\mu$-oxo $Fe^{III}$ dimer, has not been investigated. Nevertheless, some speculation on this problem has been offered. The cleavage of the O-O bond in the FeOOFe unit to form two ferryl ions, $Fe^{IV}$-O, has been frequently postulated.[2,3,4,10] Attack of $Fe^{II}$ on the oxygen atoms of the FeOOFe unit via the equation

$$FeOOFe + Fe^{II} \rightarrow FeO + FeOFe \qquad (2)$$

has been proposed, but the steric congestion required to bring three metal complexes into contact with the $O_2$ unit has also been noted as a severe drawback to such a process.[11] In con-

0002-7863/80/1502-4344$01.00/0 

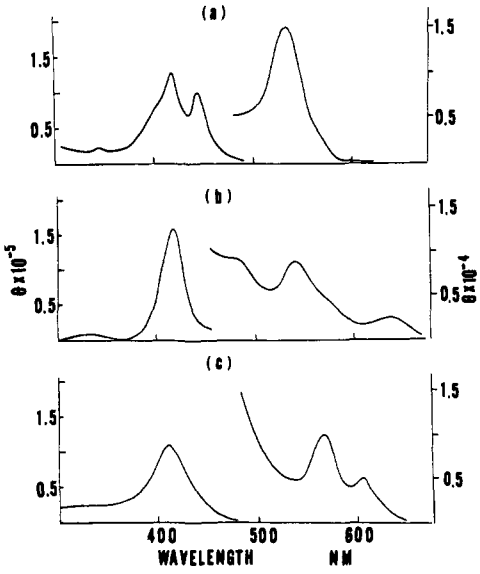


Figure 1. The visible absorption spectrum of a toluene solution of $Fe^{II}TmTP$ at 183 K: (a) under anaerobic conditions, (b) same sample as in (a) after the admission of dioxygen at 183 K, (c) same sample as in (b) after warming to 298 K and recooling to 183 K.

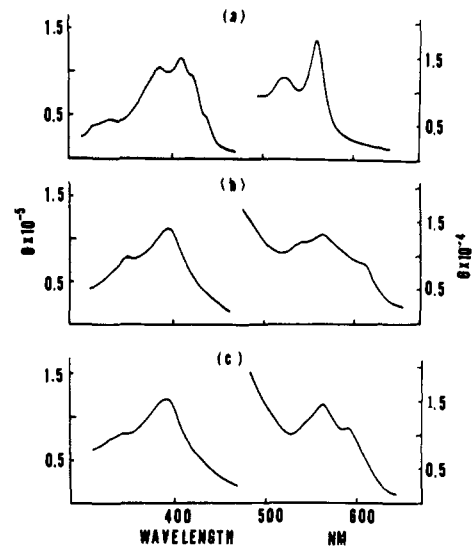


Figure 2. The visible absorption spectrum of a toluene solution of $Fe^{II}OEP$ at 183 K: (a) under anaerobic conditions, (b) same sample as in (a) after the admission of dioxygen at 183 K, (c) same sample as in (b) after warming to 298 K and recooling to 183 K.

sidering the decomposition of FeOOFe units in the solid state, the mechanism represented by eq 3 has been suggested.[11]

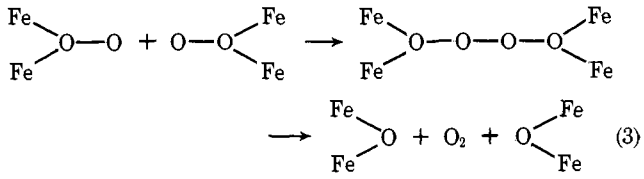


(3)

The present research has approached the problem of detecting the presumed FeOOFe unit by the use of low-temperature spectroscopic measurements in a relatively inert solution. Toluene has been chosen for reasons regarding solubility and liquid range. Under these low-temperature conditions, the rates of the reaction of reactive intermediates are slowed sufficiently so that they may be directly observed. Such techniques have been successful in detecting the reversibly formed, six-coordinate dioxygen adducts of $Fe^{II}$ porphyrins which are prepared in the presence of axial ligating bases.[12-15] For the present research, $^1H$ NMR spectroscopy has been the primary spectroscopic probe. All of the oxidation/spin states of iron either encountered in or proposed to occur in biochemical systems are paramagnetic with the exception of low-spin $Fe^{II}$. The extensive coupling between unpaired spins and porphyrin substituents produces an enormous increase in the chemical-shift range for a particular functional group. Moreover, the characteristic shift patterns for the basic oxidation/spin states of Fe porphyrin complexes have been previously determined.[16] Consequently, species with these basic oxidation/spin states are readily identified and the occurrence of species with other characteristic shift patterns must fall into new classes.

A preliminary communication dealing with some of the results described here has been published.[17]

## Results

**Spectroscopic Detection of a New Intermediate, 1, in the Autoxidation of $Fe^{II}$ Porphyrins.** Addition of dry dioxygen to a dry, degassed solution of $Fe^{II}P$ (P = a porphyrin dianion) in toluene solution at −50 °C produces an intermediate, **1**, in the autoxidation reaction. This intermediate has been observed during the oxygenation of variously substituted $Fe^{II}$ porphyrins. In referring to these differently substituted forms of **1** we will identify the porphyrin in parentheses and will use the following abbreviations: TPP, dianion of *meso*-tetraphenylporphyrin; TmTP, dianion of *meso*-tetra(*m*-tolyl)porphyrin; TpMeOPP, dianion of *meso*-tetra(*p*-methoxyphenyl)porphyrin; OEP, dianion of octaethylporphyrin; DPDMe, dianion of deuteroporphyrin IX dimethyl ester. Thus the intermediate obtained from oxygenation of $Fe^{II}TPP$ will be designated as **1**(TPP). Our observations of these species have been limited to toluene solutions. Reactions between $Fe^{II}P$ and halogenated solvents make these solvents unsuitable for oxygenation studies. Solvents such as pyridine and *N,N*-dimethylformamide, which strongly coordinate iron, alter the intrinsic reactivity of $Fe^{II}P$ so that reversibly formed dioxygen adducts are made[12] or oxidation to $(base)_2Fe^{III}P^+$ occurs.[5] Other solvents are eliminated because of insufficient solubility of $Fe^{II}P$ (e.g., saturated hydrocarbons) or by insufficient liquid range (e.g., benzene).

Optical spectral evidence for the formation of **1** is displayed in Figures 1 and 2. Trace a of Figure 1 reproduces the spectrum of $Fe^{II}TmTP$ at −80 °C under anaerobic conditions in toluene and trace b shows the spectrum of the same sample at −80 °C after the introduction of dry dioxygen. Trace c shows the spectrum obtained from this sample after allowing it to warm to 25 °C and then recooling it to −80°C. The spectrum shown in c is identical with that of the oxo-bridged dimer, TmTPFeOFeTmTP,[3,18,19] and the spectrum b is the spectrum of the intermediate **1**(TmTP). An analogous set of absorption spectra obtained from $Fe^{II}OEP$ are shown in Figure 2. The spectrum in trace b is the spectrum of **1**(OEP) and the spectrum shown as c has been identified as that of OEPFeO-FeOEP.

The $^1H$ NMR spectrum obtained after introducing dioxygen into a solution of $Fe^{II}TPP$ in toluene-$d_8$ at −80 °C is shown in Figure 3. The spectrum of **1**(TPP) shown here is distinct from the $^1H$ NMR spectra of all other previously known iron porphyrin species, although its features are grossly similar to those of TPPFeOFeTPP.[20,21] The assignments shown in the caption to Figure 3 were made by comparison with **1** obtained with other iron porphyrins. The $^1H$ NMR parameters for these related species are given in Table I. Phenyl deuteration causes an absence of the resonances in the region 7.7-7.6 ppm in the spectrum of **1**(TTP-$d_{20}$). Addition of dioxygen to solutions of $Fe^{II}OEP$ results in loss of the resonances due to $Fe^{II}OEP$ but no new resonances could be detected, although the presence of **1**(OEP) was established from visible spectroscopy. This is not unexpected since, as explained in the next section, the

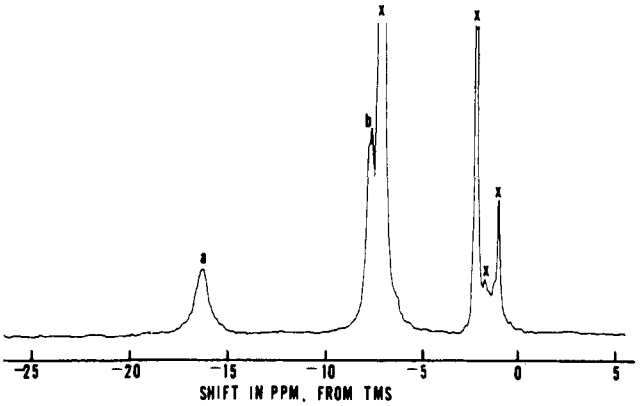


Figure 3. The $^1$H NMR spectrum of **1**(TPP) in toluene-$d_8$ at 183 K: (a) pyrrole H; (b) *o*-, *m*-, *p*-phenyl protons; (x) solvent.

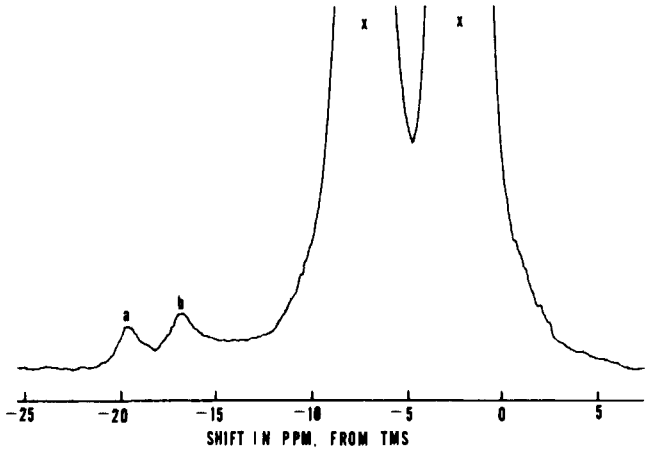


Figure 4. The $^1$H NMR spectrum of **1**(TpMeOPP) and **1**(TpMeOPP,OEP) in toluene-$d_8$ solution at 206 K formed by adding $O_2$ to a mixture of Fe$^{II}$TpMeOPP and Fe$^{II}$OEP.

resonances of **1**(OEP) are expected to be found in the regions where the solvent has strong residual absorbances. Addition of dioxygen to Fe$^{II}$DPDMe causes the disappearance of the spectrum of this species and the growth of a new resonance at −19.2 ppm (at 199 K) which we ascribe to the pyrrole protons of **1**(DPDMe). When dioxygen was admitted to a toluene-$d_8$ solution containing a mixture of Fe$^{II}$TpMeOPP and Fe$^{II}$OEP at 206°C, two resonances were detected (see Figure 4) in the region where the pyrrole protons of **1** are found. The resonance at −17 ppm is due to **1**(TpMeOPP) and we assign the resonance at −19.5 ppm to a dimer containing the two differently substituted porphyrins (i.e., **1**(TpMeOPP,OEP)).

Solutions of **1** are stable indefinitely at −80 °C (≥2 weeks) and are stable for ~1 h at −30 °C. Warming of these solutions results in the clean conversion of **1** into PFeOFeP with no other iron porphyrin complex detected by $^1$H NMR spectroscopy during the decomposition. Repeated freeze-pump-thaw cycles have demonstrated that the formation of **1** from dioxygen cannot be reversed.

The temperature dependence of the pyrrole-H isotropic shifts as a function of temperature for **1**(TmTP), **1**(DPDMe), **1**(TPMeOPP,OEP), and TmTPFeOFeTmTP is shown in Figure 5.

The magnetic susceptibility of **1**(TmTP) is temperature dependent with $\mu_{eff}$ at 2.1 $\mu_B$ at 181 K, 2.3 $\mu_B$ at 195 K, and 2.7 $\mu_B$ at 224 K.

A frozen toluene glass of **1**(TmTP) at 77 K did not produce an ESR spectrum.

**Conversion of 1 into PFeOFeP.** As indicated above, warming samples of **1** in toluene solution results in the smooth conversion of **1** into PFeOFeP with no other intermediates being detected.

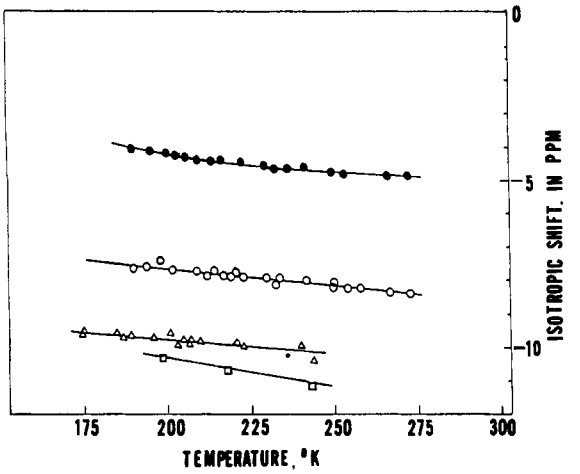


Figure 5. Graph of the pyrrole-H isotropic shift vs. temperature for (●) **1**(TmTP); (○) **1**(TPP); (△) **1**(TpMeOPP,OEP); (□) **1**(DPDMe).

Table I. $^1$H NMR Parameters (ppm) for PFeOOFeP at 193 K in Toluene-$d_8$

| porphyrin | pyrrole | *o*-, *m*-, *p*-phenyl |
|---|---|---|
| TmTP | −16.2 | −7.6, −7.7 |
| TPP | −16.0 | −7.6, −7.7 |
| TPP-$d_{20}$[b] | −16.0 | *a* |
| OEP | *a* | *a* |
| DPDMe[c] | −19.2 | *a* |

[a] No resonance observed in the characteristic region. [b] Phenyl deuterated. [c] At 199 K.

During this conversion **1** or products from **1** can act as oxidizing agents. When **1**(TmTP) is decomposed in solutions containing Fe$^{II}$TmTP the reaction

$$1 + 2Fe^{II}P \rightarrow 2PFeOFeP \quad (4)$$

occurs quantitatively as determined by monitoring the concentration of Fe$^{II}$TmTP, **1**(TmTP), and TmTPFeOFeTmTP before and after warming by $^1$H NMR spectroscopy. When **1** decomposes in the absence of Fe$^{II}$P, dioxygen is liberated quantitatively according to the equation

$$2\,1 \rightarrow 2PFeOFeP + O_2 \quad (5)$$

The dioxygen liberated has been detected by mass spectroscopy. When **1** is prepared from a mixture of principally $^{18}O_2$ and $^{16}O_2$, the isotopic composition of the dioxygen evolved is unaltered from that in the original sample. No additional $^{16}O^{18}O$ is formed. The amount of dioxygen liberated has been determined quantitatively by observing its ability to oxidize additional Fe$^{II}$TmTP to TmTPFeOFeTmTP. Thus, when a sample of **1**(TmTP) is warmed in toluene solution to room temperature and additional Fe$^{II}$TmTP is added to the sample under conditions where no dioxygen is allowed to escape from the sample, 1.0 mol of the added Fe$^{II}$TmTP is found to be oxidized for 1.0 mol of Fe$^{II}$TmTP used to originally generate **1**. However, when the sample of **1**(TmTP) is warmed to room temperature and then carefully degassed, the sample no longer has the ability to react with added Fe$^{II}$TmTP. Thus the qualitative mass spectroscopic observations and the quantitative data obtained through the use of added Fe$^{II}$TmTP are in accord that dioxygen is liberated as **1** decomposes.

During the thermal decomposition of **1**, scrambling of labeled prophyrins between dimers does occur. When a sample containing **1**(TPP) and **1**(OEP) is allowed to decompose, both TPPFeOFeTPP and the mixed dimer TPPFeOFeOEP have been detected by observation of their characteristic pyrrole-H resonances. However, no mixed form of **1** (i.e., TPPFeO$_2$FeOEP) was observed during the reaction. The formation of

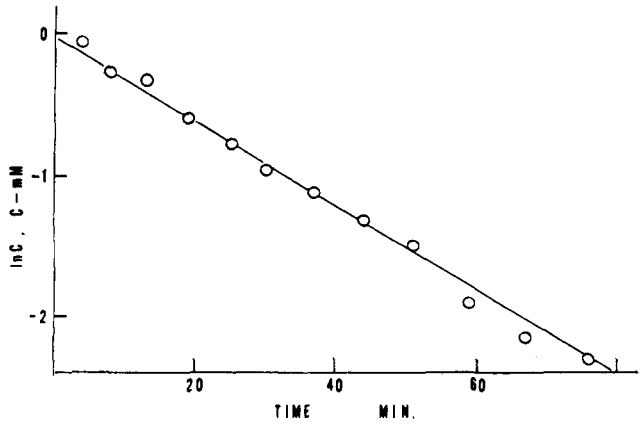


Figure 6. Plot of ln [1(TmTP)] vs. time for the thermal decomposition of 1(TmTP) in a sealed toluene-$d_8$ solution under vacuum at 246 K.

the mixed dimer, TPPFeOFeOEP, was a direct consequence of the mode of decomposition of **1**. Control experiments show that mixtures of TPPFeOFeTPP and OEPFeOFeOEP do not form TPPFeOFeOEP even after standing at 25 °C for 2 days in toluene solution.

**Kinetics of Reaction 5.** The thermal decomposition of 1(TmTP) via eq 5 was first order in **1**. Sample data for the decomposition at 246 K are plotted in Figure 6. The rate constants for decomposition of 1(TmTP) at 251 K were 0.035 ± 0.003 $min^{-1}$ when the sample was flushed with dinitrogen, 0.042 ± 0.003 $min^{-1}$ when the sample was degassed and kept under vacuum, and 0.030 ± 0.003 $min^{-1}$ when it was kept under 1 atm of dioxygen. Consequently the reaction is unaffected by the presence of dioxygen. The temperature dependence of the decomposition yields the Eyring plot shown in Figure 7. From this plot the activation parameters are $\Delta G^{\ddagger}_{298}$ = 19 ± 1 kcal/mol, $\Delta H^{\ddagger}$ = 14.5 ± 1 kcal/mol, and $\Delta S^{\ddagger}$ = −15 ± 1 eu.

## Discussion

The available evidence indicates that **1** possesses the peroxo-bridged structure $PFeO_2FeP$. The initial steps in the autoxidation of $Fe^{II}P$ then can be given by the equations

$$Fe^{II}P + O_2 \rightleftharpoons PFeO_2 \quad (6)$$

$$PFeO_2 + Fe^{II}P \rightarrow PFeO_2FeP \quad (7)$$

Thus, in the absence of a base capable of coordinating to the vacant axial site in $PFeO_2$, this species reacts with another PFe to form **1** irreversibly, whereas with amines present $BPFeO_2$ forms. $PFeO_2$ itself, however, has not been directly observed.

The stoichiometry of **1** (with one oxygen atom for each iron porphyrin) is established through the quantitative uptake of PFe by **1** via eq 4 and by the quantitative release of 0.5 mol of $O_2$ when 1 mol of **1** is converted to PFeOFeP via eq 5.

The observation that two pyrrole-H peaks are detected, one for (TpMeOPP)$FeO_2$Fe(TpMeOPP) and the other for TpMeOPP$FeO_2$FeOEP, when dioxygen is added to a mixture of $Fe^{II}$TpMeOPP and $Fe^{II}$OEP requires that **1** have a dimeric structure.

Additional proof of the dimeric nature of **1** and characterization of its electronic structure come from its $^1H$ NMR spectra and magnetic properties. The $^1H$ NMR spectra of **1** resemble those of the well-characterized $\mu$-oxo $Fe^{III}$ porphyrin dimers.[20,21] Thus **1** and PFeOFeP show pyrrole resonances in the region −10 to −20 ppm and phenyl resonances (for TPP derivatives) at ca. −8 to −7 ppm. The failure to observe the resonances of 1(OEP) in toluene is not expected in light of the $^1H$ NMR characteristics of OEPFeOFeOEP which 1(OEP) is expected to resemble. The spectrum of OEPFeOFeOEP in chloroform-$d_1$ at 29 °C shows two methylene resonances at −6.06 and −5.10 ppm and a methyl resonance at −1.75 ppm and the meso H is inferred to lie at ca. −5.3 ppm.[20] With toluene-$d_8$ as solvent these resonances lie close to or under resonances due to residual undeuterated solvent. Consequently we suspect that the resonances of 1(OEP) are obscured by solvent resonances, although the presence of **1** can be inferred because of the absence of resonances due to $Fe^{II}$OEP. The temperature dependence of the pyrrole-H contact shifts of **1** and of the magnetic susceptibility of **1** indicates that **1**, like PFeOFeP, is antiferromagnetic. Consequently a peroxo formulation ($Fe^{III}$-O-O-$Fe^{III}$) of the electronic structure is strongly favored.

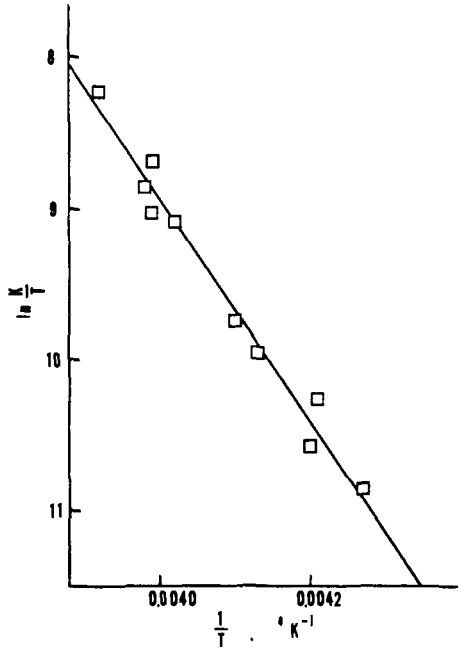


Figure 7. Eyring plot for the thermal decomposition of 1(TmTP) in toluene-$d_8$ solution.

Table II. Stoichiometry of Oxygen Evolution from **1** after Warming to 25 °C

| expt | 1[a] | 2[b] | 3[b] |
|---|---|---|---|
| aliquot A,[c] mL | 0.150 ± 0.001 | 0.071 | 0.050 |
| aliquot B,[c] mL | 0.050 | 0.100 | 0.070 |
| % P as **1** in aliquot A | 90 ± 1 | 82 | 81 |
| % P as $Fe^{II}$P in aliquots A + B | 22 | 18 | 19 |
| % P as PFeOFeP in aliquots A + B | 78 | 82 | 81 |
| [$Fe^{II}$P] from aliquot B consumed/ [**1**] in aliquot A | 0.0 | 2.0 | 2.0 |

[a] Sample was degassed before aliquot B was added. [b] Sample was *not* degassed before aliquot B was added. [c] Stock solution contains 90% $Fe^{II}$TmTP and 10% TmTPFeOFeTmTP.

The larger magnetic moment of TmTP$FeO_2$TmTP relative to TmTPFeOFeTmTP, when interpreted by a coupling between two high-spin ferric ions, indicates that an antiferromagnetic coupling $2J \sim 265$ K, which is ~30% smaller than for TmTPFeOFeTmTP.[20] The pyrrole-H contact shifts also reflect weaker coupling in **1**. The decreases in isotropic shift on lowering the temperature from 273 to 200 K are 14% for TmTPFeOFeTmTP and only 9% for **1**. The decrease in shift at lower temperature is indicative of antiferromagnetism. The weaker coupling in **1** relative to PFeOFeP can be attributed to the longer bridge in **1**.

The experimental observations reported here allow us to formulate a mechanism for the conversion of $PFeO_2FeP$ to PFeOFeP via eq 5. That mechanism, which is pertinent in a noncoordinating solvent, particularly toluene, is shown in eq 8-11.

$$PFe^{III}O_2Fe^{III}P \rightarrow 2PFe^{IV}O \quad (8)$$

$$PFe^{IV}O + PFe^{III}O_2Fe^{III}P \rightarrow PFe^{III}OFe^{III}P + O_2Fe^{II}P \quad (9)$$

$$O_2Fe^{II}P \rightleftharpoons O_2 + PFe^{II} \quad (10)$$

$$PFe^{IV}O + PFe^{II} \rightarrow PFe^{III}OFe^{III}P \quad (11)$$

$$PFe^{IV}O + O_2Fe^{II}P \rightarrow PFe^{III}OFe^{III}P + O_2 \quad (12)$$

The first step, eq 8, involves cleavage of the O-O bond to yield an $Fe^{IV}$ ferryl complex as has been proposed previously.[2,3,4,10] If this initial step is rate determining, then the decomposition of $PFeO_2FeP$ should be first order in $PFeO_2FeP$ as we have observed.[22] The occurrence of the other proposed steps is consistent with four other factors known about this system: (1) No other species is observed during the decomposition of $PFeO_2FeP$; consequently, PFeO must rapidly react with other components of the system in steps 9, 11, and 12. (2) It has been established that the isotopic composition of labeled dioxygen is not changed when it is added to $Fe^{II}P$ and then one-half of it is released as dioxygen. This requires that the O-O bond of the dioxygen which is freed has remained intact and rules out the mechanism shown in eq 3. The processes shown in eq 9 and 10 allow for maintenance of the O-O bond. (3) Labeled porphyrins do scramble between dimers during, but not subsequent to, the formation of PFeOFeP. This is allowed, and in fact required, by steps 9, 11, and 12. (4) Since these reactions are run in the absence of any ligand besides those derived from dioxygen, vacant coordination sites exist in $PFeO_2FeP$, PFe, and $PFeO_2$ and these are accessible for attack by PFeO as required by steps 9, 11, and 12. In this way the steric problems involved in getting to the $\mu$-oxo dimer are minimized. Note that the mechanisms expressed in eq 2 and 3 both require severe steric congestion.

Additional support for the cleavage of the O-O bond in eq 8 as the initial step in the decomposition of $PFeO_2FeP$ comes from our recent observations that addition of amines (B = pyridine, *N*-methylimidazole, piperidine) to $PFeO_2FeP$ generates moderately stable ferryl complexes, BPFeO.[23] Through the addition of the amine to the iron, the iron gains electron density and becomes more readily oxidizable. This in turn facilitates the formation of $Fe^{IV}$ and the breaking of the O-O bond in $PFeO_2FeP$. The ferryl complex formed via eq 8 is a more potent oxidizing agent than BPFeO since it lacks the stabilizing, electron-donating axial amine ligand and consequently its concentration never reaches detectable levels.

Other metal complexes do not necessarily follow the autoxidation path outlined for $Fe^{II}P$ in eq 8-12.[24,25] The autoxidation of low-spin, six-coordinate iron(II) porphyrins,[2,3,5,26] iron(II) in aqueous solution in the presence of $H_2PO_4^-$,[27] and $Cr(CN)_6^{-4}$ [28] appears to be a one-electron process. The outer-sphere nature of this process has been established for $Cr(CN)_6^{4-}$, where substitution-inert $Cr(CN)_6^{3-}$ is the product,[28] and for $PFe^{II}L_2$.[26] Under appropriate conditions, however, the reaction between dioxygen and iron(II) porphyrins in the presence of amines capable of occupying axial coordination sites can be converted into a reversible association process (e.g., the well-studied hemoglobin and myoglobin models).[12-14] There are several cases of metal autoxidation which do appear to have certain features in common with the path of autoxidation described here for $Fe^{II}P$. For numerous cobalt(II) complexes, the formation of peroxo-bridged, binuclear complexes occurs upon exposure to dioxygen.[8] Many of these peroxo-bridged species have been isolated as stable, crystalline substances. Unlike PFeOOFeP, they do not appear to readily convert into oxo-bridged species. The oxidation of $Pu^{III}$ in aqueous solution, like that of $Fe^{2+}$ in aqueous solution, is reported[29] to exhibit kinetic behavior which is first order in $O_2$ and second order to $Pu^{III}$ so that a peroxo-bridged intermediate is again likely. In the case of $Pu^{III}$ autoxidation, peroxide has been detected as the dioxygen reduction product. Autoxidation of $Cr^{II}$ in aqueous ammonia produces $(NH_3)_5CrOCr(NH_3)_5^{4+}$. Isotopic labeling of dioxygen has revealed that from 40 to 70% of the oxo bridge in the product was derived from the oxidant.[30] The mechanism involved here may be closely analogous to eq 8-12 with $Cr(NH_3)_5O^{2+}$ as an intermediate capable of undergoing exchange of its oxo ligand with oxygen of water. Yet another two-electron mechanism appears involved in the autoxidation of $V^{II}$.[31]

Further studies of the chemical reactivity of **1** are in progress.

## Experimental Section

**Materials.** Tetraphenylporphyrin ($H_2TPP$) and its phenyl-substituted derivatives were prepared by literature methods.[32,33] Phenyl-deuterated $H_2TPP$-$d_{20}$ was prepared from benzaldehyde-$d_5$. Octaethylporphyrin ($H_2OEP$) was a gift from Professor H. H. Inhoffen. Iron(III)chloride complexes were formed in dimethylformamide solution and the products were purified chromatographically.[34] Iron(III) deuteroporphyrin IX dimethyl ester chloride was prepared as described by Falk.[35] Unligated iron(II) porphyrin complexes were prepared either by the chromous reduction method[36] or by forming the bis(piperidine)iron(II) porphyrin complex via the route of Straub[37] and heating the solid adduct at 160 °C for 4 days to drive off the piperidine ligands.

**Instrumentation.** $^1H$ NMR spectra were obtained on a JEOL-PFT100 FT NMR spectrometer operating at 99.5 MHz in the FT mode. Between 100 and 10 000 transients were accumulated using a ~19-$\mu$s 90° pulse. A JEOL JNM-VT-3C temperature controller was utilized. Temperature calibration was carried out by measuring the peak separations of a standard methanol sample.

Electronic spectra were measured using a Cary 17 spectrometer equipped with a Kontes variable temperature Dewar. The sample was contained in a sealed cuvette with a 1-mm path length. The cuvette was cooled by immersion in an ethanol bath which was chilled by the addition of sufficient liquid nitrogen to reach the desired temperature.

Electron spin resonance measurements were made using a Varian E-4 spectrometer equipped with a liquid nitrogen cooled sample Dewar. Mass spectra were obtained using a 21-104 Consolidated Electrodynamic Corp. mass spectrometer. Spectra were obtained under the following conditions: ionizing voltage, 70 eV; anode current, 80 $\mu$A; temperature of the ionizing chamber, −250 °C. Sensitivity for peak *m/e* 32 was 666 $\mu m^{-1}$ and peak *m/e* 36 was 622 $\mu m^{-1}$.

Magnetic susceptibilities were measured by NMR using the Evans technique.[38]

**Preparation of Solution of 1.** A ~2 mM solution of iron(II) porphyrin in toluene was prepared under dry, oxygen-free nitrogen in a Kewannee controlled atmosphere drybox equipped with an inert gas purifier. The sample was sealed in a NMR tube or cuvette with a septum cap. These caps had been submersed in toluene for 24 h and then dried at 25 °C for 24 h prior to use. The sealed sample was removed from the controlled-atmosphere box and cooled to −78 °C. Dioxygen, which was dried by passage through anhydrous calcium sulfate, was introduced into the sample via a syringe needle. **1** formed after the sample container was shaken gently. Once formed, **1** is not sensitive to additional dioxygen. Although using this technique it was possible to prepare samples of **1** which are free of any other prophyrin species, some samples also contained the $Fe^{III}$ $\mu$-oxo dimer, PFeOFeP. This species formed either through incomplete deoxygenation of the original iron(II) porphyrin solution or by inadvertent warming of the solution of **1**. Since no reaction occurs between **1** and PFeOFeP and since their relative concentrations could be determined by integration of their $^1H$ NMR spectra, some experiments reported here used such solutions.

**Demonstration of the Irreversibility of Formation of 1 from Dioxygen.** The sample of **1** was prepared as described above in a Wilmad Taperlok NMR sample tube. After the sample composition had been determined at −50 °C by its $^1H$ NMR spectrum, the sample was subjected to six freeze-pump-thaw cycles using liquid nitrogen and dry ice-methanol Dewars for the freeze and thaw operations, respectively. The sample composition was again checked by its $^1H$ NMR spectrum. The intensity of the pyrrole resonance of **1** had not decreased nor had any other new peaks appeared in the spectrum.

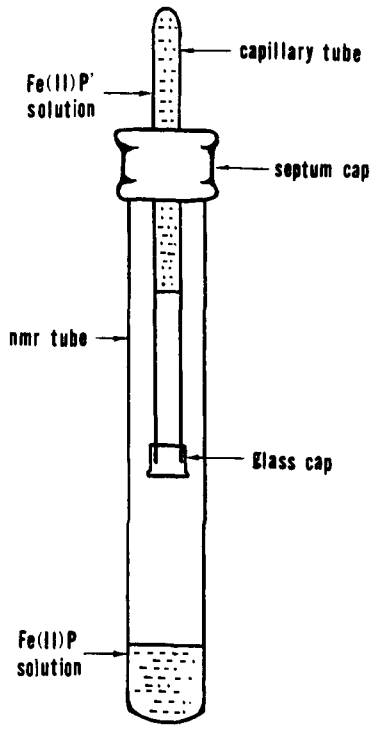


**Figure 8.** Apparatus for preparing samples of **1**(TpMeOPP) and **1**(OEP) without forming **1**(TpMeOPP,OEP).

**Decomposition of 1 in the Presence of $Fe^{II}P$.** A solution of $Fe^{II}TmTP$ in toluene in a sealed NMR tube was prepared and cooled to −78 °C as described above. A small quantity (ca. 2 μL) of dioxygen which was sufficient to convert only part of the $Fe^{II}P$ to **1** was introduced into the sample via a syringe. The NMR tube was shaken while in the dry ice–methanol bath to ensure complete reaction of all dioxygen. At −50 °C the relative concentrations of $Fe^{II}P$, **1**, and PFeOFeP were determined from the integrated intensities of the ortho protons of $Fe^{II}P$ at −26 ppm, the meta and para protons of $Fe^{II}P$ at −14.5 ppm, the pyrrole protons of **1** at −16 ppm, and the pyrrole protons of PFeOFeP at −13 ppm. The solution was allowed to warm to room temperature. Then it was cooled to −50 °C and the relative concentrations of $Fe^{II}P$, **1**, and PFeOFeP were redetermined. For two independent samples the following data were obtained. Original samples 1: $Fe^{II}P$, 49 ± 1%; **1**, 34 ± 1%; PFeOFeP, 17 ± 1%. Sample 1 after warming: $Fe^{II}P$, 15 ± 1%; **1**, 0%; PFeOFeP, 85 ± 1%. Original sample 2: $Fe^{II}P$, 53 ± 1%; **1**, 32 ± 1%; PFeOFeP, 15 ± 1%. Sample 2 after warming: $Fe^{II}P$, 22 ± 1%; **1**, 0%; PFeOFeP, 78 ± 1%. These percentages are expressed as percent of all iron porphyrin present. Thus the stoichiometry of reaction is $2Fe^{II}P + 1 = 2PFeOFeP$.

**Mass Spectroscopy of the Gas Evolving from 1 on Thermal Decomposition.** A 5-mL solution containing 2 mM $Fe^{II}TmTP$ was prepared in a sealed tube. Approximately 2 mL of a mixture of isotopically labeled dioxygen (which had the composition 54.9% $^{18}O_2$, 1.0% $^{18}O^{16}O$, 44.1% $^{16}O_2$) was introduced into the sample after it had been cooled to −78 °C in a dry ice–methanol bath. The sample was agitated to ensure complete formation of **1**. The sample tube was connected to the inlet vacuum line of the mass spectrometer through a stopcock and a ground glass joint, and the sample itself frozen in liquid nitrogen. The sample was cycled through freeze-pump-thaw operations using liquid nitrogen and dry ice–methanol baths until no inlet gas was detected by the mass spectrometer. Before the inlet gas was sampled, the sample solution was frozen in liquid nitrogen. The sample was sealed off, warmed to room temperature, and then refrozen in liquid nitrogen. After this operation the gas produced by the warming was sampled by the mass spectrometer. Dioxygen in concentrations well above the machine background was detected in the inlet gases. The isotopic composition of the dioxygen produced was 53.0% $^{18}O_2$, 1.2% $^{18}O^{16}O$, 45.8% $^{16}O_2$.

**Porphyrin Scrambling during Decomposition.** The apparatus shown in Figure 8 was designed to allow solutions of $TPPFeO_2FeTPP$ and $OEPFeO_2FeOEP$ to be prepared. In an inert atmosphere a toluene solution of $Fe^{II}TPP$ was placed in the NMR tube and a toluene solution of $Fe^{II}OEP$ was placed in the capillary tube. After the NMR tube was cooled in a dry ice–methanol bath a small quantity of dry dioxygen was introduced into the tube via a syringe through the septum cap and the tube was shaken and then purged with dry dinitrogen. The syringe needle was then used to remove the glass cap and the solution from the capillary tube was mixed into the solution in the NMR tube. More dry dioxygen was added to the sample via a syringe. The $^1H$ NMR spectrum of the mixture at −50 °C exhibited the characteristic pyrrole resonance of $TPPFeO_2FeTPP$, but the previously characterized resonance due to $TPPFeO_2FeOEP$ was completely absent. The sample was warmed to room temperature. Since the temperature dependence of the pyrrole protons of TPPFeOFeTPP and TPPFeOFeOEP causes them to overlap at 25 °C, the sample was cooled to −50 °C and its $^1H$ NMR spectrum was recorded. In addition to the pyrrole resonance of TPPFeOFeTPP at −12.5 ppm, a second resonance at −13.5 ppm due to the pyrrole protons of TPPFeOFeOEP was resolved. A mixture of TPPFeOFeTPP and OEPFeOFeOEP in toluene solution did not display the resonance at −13.5 ppm when cooled to −50 °C after standing at 25 °C for 2 days.

***Kinetics of Thermal Decomposition of 1.*** Samples of ***1***(*TmTP*) were prepared as described above and were allowed to autodecompose in the probe of the NMR instrument at a fixed, controlled temperature. The reaction was monitored by determining the relative concentrations of **1** and PFeOFeP by integration of their pyrrole-proton resonances. The total iron porphyrin concentration was obtained by warming the sample to room temperature, whereupon it was entirely converted to PFeOFeP. The final concentration of PFeOFeP was determined spectrophotometrically.

**Acknowledgments.** We thank the National Institutes of Health (GM26226, HL 16087) for generous support and Dr. J. Del Gaudio for assistance in the early phases of this work.

## References and Notes

(1) For a detailed review on the interaction of dioxygen and metalloporphyrins and related species see: James, B. R. In "The Porphyrins", Dolphin, D.,
(2) Kao, O. H. W.; Wang, J. H. *Biochemistry* **1965**, *4*, 342–347.
(3) Cohen, I. A.; Caughey, W. S. *Biochemistry* **1968**, *7*, 636–641.
(4) Hammond, G. S.; Wu, C.-H. S. *Adv. Chem. Ser.* **1968**, *77*, 186–207.
(5) Alben, J. O.; Fuchman, W. H.; Beaudreau, C. A.; Caughey, W. S. *Biochemistry* **1968**, *7*, 624–635.
(6) Kurtz, Jr., D. M.; Shriver, D. F.; Klotz, I. M. *Coord. Chem. Rev.* **1977**, *24*, 145–178.
(7) Baldwin, J. E.; Huff, J. *J. Am. Chem. Soc.* **1973**, *95*, 5757–5759.
(8) McLendon, G.; Martell, A. E. *Coord. Chem. Rev.* **1976**, *19*, 1–39.
(9) Erskin, R. W.; Field, B. O. *Struct. Bonding (Berlin)* **1976**, *28*, 1–50.
(10) Collman, J. P. *Acc. Chem. Res.* **1977**, *10*, 265–272.
(11) Niswander, R. H.; Martell, A. E. *Inorg. Chem.* **1978**, *17*, 2341–2344.
(12) Weschler, C. J.; Anderson, D. L.; Basolo, F. *J. Am. Chem. Soc.* **1975**, *97*, 6707–6713.
(13) Wagner, G. C.; Kassner, R. J. *J. Am. Chem. Soc.* **1974**, *96*, 5593–5595.
(14) Brinigar, W. S.; Chang, C. K.; Geibel, J.; Traylor, T. G. *J. Am. Chem. Soc.* **1974**, *96*, 5597–5599.
(15) Almog, J.; Baldwin, J. E.; Dyer, R. L.; Huff, J.; Wilkerson, C. J. *J. Am. Chem. Soc.* **1974**, *96*, 6000–6001.
(16) La Mar, G. N.; Walker, F. A. In ref 1, 1979; Vol. IV, Part B, pp 61–157.
(17) Chin, D.-H.; Del Gaudio, J.; La Mar, G. N.; Balch, A. L. *J. Am. Chem. Soc.* **1977**, *99*, 5486–5488.
(18) Cohen, I. A. *J. Am. Chem. Soc.* **1969**, *91*, 1980–1983.
(19) Fleischer, E. B.; Srivastava, T. S. *J. Am. Chem. Soc.* **1969**, *91*, 2403–2405.
(20) La Mar, G. N.; Eaton, G. R.; Holm, R. H.; Walker, F. A. *J. Am. Chem. Soc.* **1973**, *95*, 63–75.
(21) Wicholas, M.; Mustacich, R.; Jayne, D. *J. Am. Chem. Soc.* **1972**, *94*, 4518–4522.
(22) The negative value of the entropy of activation for this reaction may result from solvation effects occurring during the conversion of the dimeric **1** to monomeric PFeO.
(23) Chin, D. H.; Balch, A. L.; La Mar, G. N. *J. Am. Chem. Soc.* **1980**, *102*, 1446–1448.
(24) Taube, H. *J. Gen. Physiol.* **1969**, *49*, 29–50.
(25) Fallab, S. *Angew. Chem., Int. Ed. Engl.* **1967**, *6*, 496–507.
(26) Chu, M. M. L.; Castro, C. E.; Hathaway, G. M. *Biochemistry* **1978**, *17*, 481–486.
(27) Cher, M.; Davidson, N. *J. Am. Chem. Soc.* **1955**, *77*, 793–798.
(28) Haim, A.; Wilmarth, W. K. *J. Am. Chem. Soc.* **1961**, *83*, 509–516.
(29) Newton, T. W.; Baker, F. B. *J. Phys. Chem.* **1958**, *60*, 1417–1421.
(30) Joyner, T. B.; Wilmarth, W. K. *J. Am. Chem. Soc.* **1961**, *83*, 516–520.
(31) Swinehart, J. H. *Inorg. Chem.* **1965**, *4*, 1069–1070.
(32) Adler, A. D.; Longo, F. R.; Finareli, J. F.; Goldmacher, J.; Assour, J.; Korsakoff, L. *J. Org. Chem.* **1967**, *32*, 476.
(33) Adler, A. D.; Longo, F. R.; Kampus, F.; Kim, J. *J. Inorg. Nucl. Chem.* **1970**,

32, 2443-2445.
(34) Walker, J. A.; La Mar, G. N. *Ann. N.Y. Acad. Sci.* **1973**, *206*, 328-348.
(35) Falk, J. E. "Porphyrins and Metalloporphyrins"; Elsevier: Amsterdam, 1964; p 179.
(36) Collman, J. P.; Reed, C. A. *J. Am. Chem. Soc.* **1973**, *95*, 2048-2049.
(37) Epstein, L. M.; Straub, D. K.; Maricondi, C. *Inorg. Chem.* **1967**, *6*, 1720-1724.
(38) Evans, D. F. *J. Chem. Soc.* **1959**, 2003-2005.

# Electron Exchange Kinetics of $[Fe_4S_4(SR)_4]^{2-}/[Fe_4S_4(SR)_4]^{3-}$ and $[Fe_4Se_4(SR)_4]^{2-}/[Fe_4Se_4(SR)_4]^{3-}$ Systems. Estimates of the Intrinsic Self-Exchange Rate Constant of 4-Fe Sites in Oxidized and Reduced Ferredoxins

**John G. Reynolds, Catherine L. Coyle,[1] and R. H. Holm***

*Contribution from the Department of Chemistry, Stanford University, Stanford, California 94305.* *Received November 8, 1979*

**Abstract:** The electron self-exchange kinetics for the systems $[Fe_4S_4(SR)_4]^{2-,3-}$ (R = $CH_2Ph$, $p$-$C_6H_4Me$) and $[Fe_4Se_4(S$-$p$-$C_6H_4Me)_4]^{2-,3-}$ have been determined by general line shape analysis of exchange-broadened $^1H$ NMR spectra in acetonitrile solution. Reactions are second order, first order each in oxidized and reduced clusters, and at 300-304 K rate constants fall in the interval $10^6$-$10^7$ $M^{-1}$ $s^{-1}$, placing them among the faster inorganic self-exchange systems. For the $[Fe_4S_4(S$-$p$-$C_6H_4Me)_4]^{2-,3-}$ electron exchange $k_{301K}(obsd) = 2.8 \times 10^{-6}$ $M^{-1}$ $s^{-1}$ with activation parameters $\Delta H^{\ddagger} = 3.6$ kcal/mol and $\Delta S^{\ddagger} = -17$ eu. The structural reorganization energy of $Fe_4S_4$ cores upon passing from a compressed tetragonal to an elongated tetragonal geometry via a proposed $T_d$ transition state in an outer-sphere process is estimated to be $\Delta G^{\ddagger}_{reorg} \sim 1.4$ kcal/mol. The rate constants are the best current estimates of the intrinsic values for the $[Fe_4S_4(S$-$Cys)_4]$ redox sites of ferredoxins in the couple $Fd_{ox}/Fd_{red}$, for which $[Fe_4S_4(SR)_4]^{2-}$ and $[Fe_4S_4(SR)_4]^{3-}$ serve as synthetic analogues of the sites of oxidized and reduced proteins, respectively. The "slow" electron self-exchange rates on the NMR time scale between oxidized and reduced forms of proteins containing one 4-Fe site can now be primarily attributed to kinetically retarding steric influences of protein structure rather than intrinsically slow reactions of the sites themselves.

## Introduction

The principal physiological functions of that class of iron-sulfur proteins known as ferredoxins (Fd) is electron transfer, wherein these proteins serve as components of electron-transport chains coupled to a wide variety of "ferredoxin-dependent" oxidoreductases.[2] In this function many ferredoxins appear to operate through the $Fd_{ox}/Fd_{red}$ couple

$$[Fe_4S_4(S\text{-}Cys)_4]^{2-}\ (Fd_{ox}) + e^- \rightleftharpoons [Fe_4S_4(S\text{-}Cys)_4]^{3-}\ (Fd_{red}) \quad (1)$$

in the case of proteins containing 4-Fe sites. Required information for an ultimately satisfactory interpretation of the functional operation of ferredoxins is accurate values of potentials and electron exchange rates and identification of those factors, intrinsic and extrinsic to the redox site, which significantly influence these quantities. One set of such factors which is expected to affect both equilibrium and kinetic aspects of protein behavior are the structures of the oxidized and reduced forms. Although the structures of *Peptococcus aerogenes* $Fd_{ox}$[3] and the reduced "high-potential" protein from *Chromatium*[3bc] ($HP_{red}$), which contain isoelectronic 4-Fe sites, are rather well defined from protein crystallography, no structure of a $Fd_{red}$ protein is available. Further, no electron-exchange rates for $Fd_{ox}/Fd_{red}$ are available other than certain estimated values (vide infra). Our approach to elucidation of the operation of Fd 4-Fe redox sites utilizes well-characterized synthetic analogues of these sites.[4,5]

Extensive physicochemical investigations of the oxidized cubane-type clusters $[Fe_4S_4(SR)_4]^{2-}$ [4-10] and their one-electron reduction products, $[Fe_4S_4(SR)_4]^{3-}$,[11-15] have demonstrated that these species are analogues of the 4-Fe clusters in $Fd_{ox}$ and $HP_{red}$, and $Fd_{red}$, respectively. Recently, related selenium-containing clusters $[Fe_4X_4(YPh)_4]^{2-}$ (X, Y = S, Se), have been prepared in this[16] and another laboratory,[17] and their reduced forms generated in solution.[16] Among the characterized features of oxidized and reduced clusters are their structures and $^1H$ NMR spectral properties. The structures of $[Fe_4S_4(SPh)_4]^{2-}$,[7] $[Fe_4S_4(SPh)_4]^{3-}$,[13] $[Fe_4S_4(SCH_2Ph)_4]^{2-}$,[6] $[Fe_4S_4(SCH_2Ph)_4]^{3-}$,[15] and $[Fe_4Se_4(SPh)_4]^{2-}$ [16] are of particular pertinence to the present investigation and are summarized in Figure 1. In comprehensive studies of crystalline and solution-state properties of clusters, it has been demonstrated that the process

$$[Fe_4S_4(SR)_4]^{2-} \underset{-e^-}{\overset{+e^-}{\rightleftharpoons}} [Fe_4S_4(SR)_4]^{3-} \quad (2)$$

(I, compressed $D_{2d}$) (II, elongated $D_{2d}$)

schematically depicted in Figure 1, represents the essential $Fe_4S_4$ core structural change accompanying electron transfer between oxidized and reduced clusters when extrinsic structural constraints are minimized.[13,14] The rather small structural differences between the two oxidation states suggest high electron self-exchange rates. In order to define exchange rates of clusters, measurements have been conducted for the pairs $[Fe_4S_4(S$-$p$-$C_6H_4Me)_4]^{2-,3-}$, $[Fe_4S_4(SCH_2Ph)_4]^{2-,3-}$, and $[Fe_4Se_4(S$-$p$-$C_6H_4Me)_4]^{2-,3-}$ in acetonitrile solution. Employment of NMR line shape analysis used for the kinetic measurements is facilitated by the large differences in $^1H$ chemical shifts, predominantly effected by isotropic contact interactions,[8-10,12] between the oxidized and reduced clusters. The results of this investigation, together with earlier measurements of comparative $Fd_{ox,red}/[Fe_4S_4(SR)_4]^{2-,3-}$ potentials[18] and the demonstration of process 2,[13,14] contribute to an emerging picture of the intrinsic operation of 4-Fe clusters in electron transfer, i.e., in the absence of modulating influences of protein structure.

0002-7863/80/1502-4350$01.00/0 